Geographic Distribution and Relative Abundance of the Invasive Glassy-Winged Sharpshooter: Effects of Temperature and Egg Parasitoids

Author(s): Andrew Paul Gutierrez, Luigi Ponti, Mark Hoddle, Rodrigo P.P. Almeida, and Nicola A. Irvin

Geographic Distribution and Relative Abundance of the Invasive Glassy-Winged Sharpshooter: Effects of Temperature and Egg Parasitoids

ANDREW PAUL GUTIERREZ,[1,2] LUIGI PONTI,[1,3] MARK HODDLE,[4] RODRIGO P.P. ALMEIDA,[5] AND NICOLA A. IRVIN[4]

ABSTRACT The capacity to predict the geographic distribution and relative abundance of invasive species is pivotal to developing policy for eradication or control and management. Commonly used methods fall under the ambit of ecological niche models (ENMs). These methods were reviewed and shortcomings identified. Weather-driven physiologically based demographic models (PBDMs) are proposed that resolve many of the deficiencies of ENMs. The PBDM approach is used to analyze the invasiveness of the polyphagous glassy-winged sharpshooter (*Homalodisca vitripennis* [Germar]), a pest native to the southeastern United States and northeastern Mexico that extended its range into California in 1989. Glassy-winged sharpshooter vectors the pathogenic bacterium, *Xylella fastidiosa* (Wells) that causes Pierce's disease in grape and scorch-like diseases in other plants. PBDMs for glassy-winged sharpshooter and its egg parasitoids (*Gonatocerus ashmeadi* Girault and *G. triguttatus* Girault) were developed and linked to a PBDM for grape published by Wermelinger et al. (1991). Daily weather data from 108 locations across California for the period 1995–2006 were used to drive the PBDM system, and GRASS GIS was used to map the simulation results. The geographic distribution of glassy-winged sharpshooter, as observed, is predicted to be largely restricted to the warm areas of southern California, with the action of the two egg parasitoids reducing its abundance >90%. The average indispensable mortality contributed by *G. triguttatus* is <1%. A temperature-dependent developmental rate model for *X. fastidiosa* was developed that suggests its geographic range is also limited to the warm inland areas of southern California. Biological control of glassy-winged sharpshooter further decreases the pathogen's relative range. Climate warming scenarios of +2°C and +3°C suggest that the distribution and severity of glassy-winged sharpshooter and *X. fastidiosa* will increase in the agriculturally rich central valley of California. The utility of holistic analyses for formulating control policy and tactics for invasive species is discussed.

KEY WORDS grape, glassy-winged sharpshooter, *Homalodisca vitripennis*, invasive species, GIS

Invasive species cause in excess of $140 billion in losses annually in the United States (Pimentel et al. 2000). Experience suggests these problems are often handled in a crisis mode by state and federal agencies that lack the capacity to predict the potential geographic range and relative abundance of invasive species under current and climate change scenarios. This capacity is pivotal to developing sound policy for their eradication or control and management. Predicting the geographic distribution and dynamics of invasive species in time and space has been a difficult recurring problem (Mills and Getz 1996), and the complexity may increase with global climate change.

It is well known that the local phenology, dynamics, and abundance of ectothermic species are largely determined by weather and interacting species, with climate (i.e., long run weather) and interacting species determining the native geographic range (Andrewartha and Birch 1954, Walther 2002, Wellington et al. 1999). Examples of the effects of weather (principally temperature) on invasive species and their biological control include cottony cushion scale (*Icerya purchasi* Maskell) (Quezada and DeBach 1973), olive scale (*Parlatoria oleae* (Colvée)) (Huffaker and Kennett 1966, Rochat and Gutierrez 2001), klamath weed (*Hypericum perforatum* L) (Huffaker and Kennett 1959), and red scale (*Aonidiella aurantii* (Maskell)) (DeBach and Sundby 1963).

Among the methods used to predict the geographic distribution of species are ecological niche models (ENMs). ENMs may be physiological index models (Fitzpatrick and Nix 1968, Gutierrez et al. 1974,

[1] Center for the Analysis of Sustainable Agricultural Systems (CASAS Global), 37 Arlington Ave., Kensington, CA, USA 94707.
[2] Corresponding author: Division of Ecosystem Science, College of Natural Resources, University of California, 329 Mulford Hall, Berkeley, CA 94720-3114 (e-mail: CASAS.Global@berkeley.edu).
[3] Laboratorio Gestione Sostenibile degli Agro-Ecosistemi (UTAGRI-ECO), Agenzia nazionale per le nuove tecnologie, l'energia e lo sviluppo economico sostenibile (ENEA), Centro Ricerche Casaccia, Via Anguillarese 301, 00123 Roma, Italy.
[4] Department of Entomology, University of California, Riverside, CA 92521.
[5] USA Department of Environmental Science Policy and Management, University of California, Berkeley, CA 94720-3114.

Sutherst et al. 1991), statistical models (e.g., generalized linear models, generalized additive models, generalized boosted models, genetic algorithm for rule-set prediction, principal components analysis (see Estrada-Peña 2008, Mitikka et al. 2008), or models based on artificial intelligence concepts (Phillips et al. 2006). These approaches attempt to characterize the ecological niche of a species based on weather and other factors in the species' native range, and then to use the ENM to estimate the potential invasiveness of the species in new areas. Deficiencies of ENMs include difficulty incorporating trophic interactions (Davis et al. 1998), aggregate weather data may be used that miss important short-term weather effects, the assumed native range may be in error, and different ENM approaches may give different results.

Many of these deficiencies may be resolved using physiologically based demographic models (PBDMs) that may include the bottom-up effects of plant growth and development, and the top-down action of natural enemies (e.g., Gutierrez et al. 2005, 2007, 2009, 2010, Ponti et al. 2009). Instead of beginning with the assumed native range of an invasive species, PBDMs capture the weather-driven biology and population dynamics of the invasive species and of its interacting species. Observed daily weather or climate scenarios are used to drive the model dynamics of the species of interest across time and geographic space.

In this paper, we use the invasive glassy-winged sharpshooter, *Homalodisca vitripennis* (Germar) in California to explore the utility of the PBDM approach. We first review glassy-winged sharpshooter in California.

Glassy-Winged Sharpshooter Invasion of California

Glassy-winged sharpshooter is a polyphagous subtropical-tropical species native to the southeastern United States and northeastern Mexico (Adlerz 1980, Triapitsyn and Phillips 2000, Turner and Pollard 1959) that extended its range into California in 1989 (Sorensen and Gill 1996). Glassy-winged sharpshooter and native leafhoppers vector the pathogenic bacterium, *Xylella fastidiosa* (Wells et al. 1987), that causes Pierce's disease (PD) in grape (*Vitis vinifera* L.) and scorch-like diseases in other plants (e.g., oleanders and almonds) (Hopkins and Purcell 2002, Purcell 1997). Different grape varieties are cultivated in different ecological zones of California. Before the invasion of glassy-winged sharpshooter, outbreaks of PD occurred in coastal and central California vineyards (Redak et al. 2004). Increases of PD in southern California have been attributed to glassy-winged sharpshooter (Almeida and Purcell 2003, Purcell and Saunders 1999).

Glassy-winged sharpshooter develops on numerous host plants (Lauzière and Sétamou 2009) where it feeds on nutrient-poor xylem (Mizell et al. 2008). Two or more generations per year occur in southern California (Blua et al. 2001, Turner and Pollard 1959). Glassy-winged sharpshooter lacks a diapause stage with development continuing throughout the year as weather and host plant conditions allow. Glassy-winged sharpshooter normally overwinter as reproductively inactive adults (Hummel et al. 2006, Turner and Pollard 1959) with adults able to fly at ambient air temperatures >11°C and feed at temperatures >13.3°C (see Johnson et al. 2006). Citrus is a major overwintering host in California (Perring et al. 2001).

To limit the spread of glassy-winged sharpshooter, an area-wide control program using insecticides and quarantine was implemented (California Department of Food and Agriculture [CDFA] 2005), with a successful biological control program using egg parasitoids (*Gonatocerus ashmeadi* Girault (GA) and *G. triguttatus* Girault (GT)) (both Hymenoptera: Mymaridae) initiated in 2000 (Pilkington et al. 2005). GA was likely self-introduced (Vickerman et al. 2004), but was also mass reared and redistributed by the CDFA. Sporadic establishment of GT in southern California occurred because of the CDFAs classical biological control program (Pilkington and Hoddle 2007a, 2007b). Despite these control efforts, glassy-winged sharpshooter established in southern California and the southern Central Valley (Blua et al. 2001), and has been detected in north central California (CDFA 2003).

The goals of our study were to assess the potential distribution and relative abundance of glassy-winged sharpshooter, its parasitoids and Pierce's disease in California, and to examine the biological control of glassy-winged sharpshooter by GA and GT. We also examine the hypothetical effects of a warmer climate on glassy-winged sharpshooter distribution and abundance. To do this, we developed a holistic PBDM system of the interactions of grapevine, glassy-winged sharpshooter, and its egg parasitoids.

Method

The System Model for Grape, Glassy-Winged Sharpshooter, and Two-Egg Parasitoids. The system model is modular consisting of sixteen ($n = 1, 16$) linked functional age-structured population dynamics models that may be in units of numbers, mass or both. Each sub-model is based on the distributed maturation-time dynamics model proposed by Vansickle (1977, see appendix). Wermelinger et al. (1991) developed the grapevine model we used. It is a canopy model consisting of subunit models for the mass of leaves ($n = 1$), stem (2), shoots (3), and root (4), and the mass and number of fruit clusters (5, 6). The models for glassy-winged sharpshooter consist of age-mass structured models for unparasitized eggs (7, 8), nymphs (9, 10), and adults (11, 12). Each parasitoid model consists of submodels for immature stages in parasitized eggs and for free-living adults [GA (13, 14); GT (15, 16)]. The underpinning modeling concepts are found in Gutierrez and Baumgärtner (1984) and Gutierrez (1992), and the mathematics of the time-invariant and time-varying distributed maturation-time dynamics models used here are found in Vansickle (1977), Gutierrez (1996), and DiCola et al. (1999). A brief review of the dynamics model is pre-
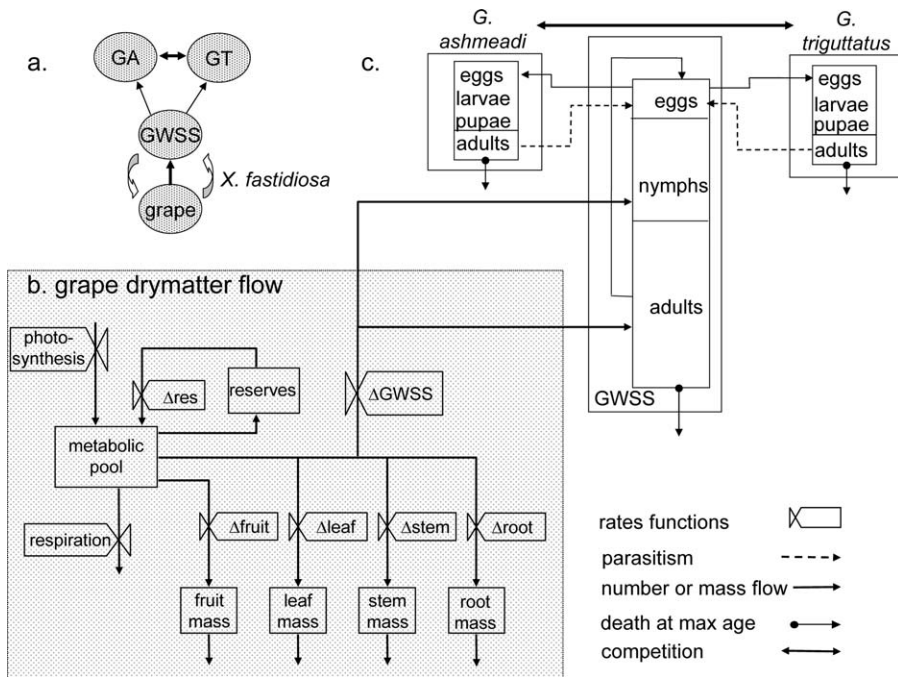
Fig. 1. The biology of the grape/glassy-winged sharpshooter/pathogen/two parasitoid system: (a) the basic tri-trophic relationships, (b) dry matter flow in grape and to glassy-winged sharpshooter, and (c) the stage specific relationships between glassy-winged sharpshooter and its two parasitoids (*G. ashmeadi* (GA) and *G. triguttatus* (GT)).

sented in the appendix. The model for the pathogen *X. fastidiosa* is a temperature-dependent developmental (growth) rate model. The time step in all of the dynamics models is a day of variable length in physiological time units as appropriate for each species, stage, or both.

Data from the literature used to formulate and parameterize the models were of varying degrees of completeness and quality, and reinterpretation of the data and judgment in their use were required. The biology summarized below was incorporated in the system model (see Appendix).

Grape. The model for grapevine (variety *chenin blanc*) (Wermelinger et al. 1991) was used without modification to capture the bottom-up plant effects on glassy-winged sharpshooter, the egg parasitoids, and their interactions (Fig. 1a). The effects of PD on grape were not included in the system model (see below). The model captures the phenology of winter dormancy, bud break, veraison and harvest, and dry matter growth and development of vegetative and fruit sub units. The flow of energy (dry matter) in the system is illustrated in Fig. 1b. Water and nutrients are assumed nonlimiting, and hence only daily maximum and minimum temperatures and solar radiation (cal cm^{-2} d^{-1}) are required for the plant. Full details of the grape model are found in Wermelinger et al. (1991, see also Gutierrez et al. 1985), and hence the model is not reviewed further.

Glassy-Winged Sharpshooter. The biology of glassy-winged sharpshooter and its two-egg parasitoids is illustrated in Figs. 1b and c. Among the factors esti-

mated for the insect species were temperature thresholds, nonlinear temperature-dependent developmental rate functions, duration of life stages, maximum per capita age-specific fecundity, temperature-dependent scalars for reproduction and longevity, temperature-dependent mortality rates, and sex ratios (Table 1).

Rate of development of glassy-winged sharpshooter. The effects of temperature (T) on the rate of development of all of the species in the system, including the pathogen, were modeled using equation 1 (Brière et al. 1999). This model has a minimum number of parameters: constants a and b, a lower threshold (θ_L), and an upper threshold (θ_U) where the function begins to decline to zero.

The rate of development of the glassy-winged sharpshooter egg stage ($R_{GW,egg}(T) = 1/days$) was estimated in the range 16.7–35°C (Al-Wahaibi and Morse 2003) (Fig. 2a) yielding thresholds $\theta_L = 11.9$°C and $\theta_U = 35.75$°C.

$$R_{GW,egg}(T) = \frac{a - (T - \theta_L)}{1 + b^{(T - \theta_U)}}$$

$$= \frac{0.0085(T - 11.9)}{1 + 2.4^{T - 35.75}} \qquad [1]$$

$R_{GW,egg}(T)$ was scaled for use for all other glassy-winged sharpshooter life stages because data for them were unavailable.

Glassy-winged sharpshooter longevity. Using data from Sétamou and Jones (2005) and the lower threshold θ_L (equation 1), we estimated the average devel-

Table 1. Parameters for the glassy-winged sharpshooter/parasitoid/disease system

Function	Parameter	GWSS	G. ashmeadi	G. triguttatus	X. fastidiosa
Rate of development at temp T	a	0.0085^a	0.005^b	0.005^c	0.00865^e
$R(T) = a(T - \theta_L)/(1 + b^{(T-\theta_U)})$	θ_L	11.9	9.25	10.5	12.5
	b	2.4	4.5	4	2.75
	θ_U	35.75	33.85	34.1	32.25
Duration of life stages (dd)		Egg $(107.5)^f$	Egg-pupae $(198)^{b,c}$	Egg-pupae $(204)^d$	
		Nymphs $(792\psi_N)$	Adult ♀ $(241\psi_{GA})$	Adult ♀ $(222\psi_{GT})$	
		Preovip (216)	(see text for ψ_{GA})	(see text for ψ_{GT})	
		Repro-adults $(1660\psi_P)$			
		See text for ψ_N, $\psi_P{}^g$			
Temp scalars	T_{min}	15.86^h	$12.5^{b,c}$	14.5^d	
$\phi_T = 1 - \left[\dfrac{T - T_{min} - T_{mid}}{T_{mid}}\right]$	T_{max}	32.5	34.5	34	
Max age ($x = dd$) specific per capita fecundity/d at 27°C		$\dfrac{0.167x_{fh}}{1,0029^x}$	$\phi_{T,GA} \cdot 110e^{-0.0161xb}$	$\phi_{T,GT} \cdot 110e^{-0.0273xd}$	
Preoviposition period		216 dd^f	<1 d	<1 d	
Sex ratio (females /males)		$1{:}1^f$	$2{:}1^b$	$2{:}1^d$	
Egestion rate[i]	β	0.83	—	—	
Demand rate (mg d^{-1})[j]	Nymphs	$(0.0003e^{0.006x}) \cdot \Delta dd$	—	—	
	Adults	$(0.0003e^{0.006(x=792)}) \cdot \Delta dd$	—	—	
Respiration rate (mg $mg^{-1}d^{-1}$)[i]	Nymphs-adults	$0.1 \times 2^{0.1 \cdot T}$	—	—	
Delay parameter k[i]		25	25	25	

[a] Al-Wahaibi and Morse 2003, [b] Pilkington and Hoddle 2006a, [c] Chen et al. 2006a, [d] Pilkington and Hoddle 2007a, [e] Feil and Purcell 2001, [f] Sétamou and Jones 2005, [g] Son et al. 2009, [h] Johnson et al. 2006, and Leopold et al. 2004, [i] A. P. Gutierrez (assumption), [j] Brodbeck et al. 2004.

opmental times in dd for nymphs ($\Delta_N = 792 \, dd_{>11.9°C}$) and adults ($\Delta_A = 1,876 \, dd_{>11.9°C}$) (Table 1). Son et al. (2009, equation 2 estimated the mean time in days (d) to 50% adult survivorship (i.e., mortality) at different temperatures, with 81.75 d at 25.25°C ($=T_{max}$) being the maximum. Normalizing the data, average adult survivorship declines with age (Fig. 2b), and is concave on temperature ($0 \le \psi_{GW}(T) \le 1$) with the maximum at T_{max} and zero at 0 and 40°C (Fig. 2c, equation 2i with parameters $\rho_1 = \rho_2$).

$$\psi_{GW}(T) = \exp[1 + (T_{max} - T)/(-\rho_1) - e^{(T_{max}-T)/(-\rho_2)}]$$

$$= \exp[1 + (25.25 - T)/(-7.05)$$

$$- e^{(25.25-T)/(-7.05)}] \qquad [2i]$$

Expected average nymph and adult longevity (subscripts N and A) change daily with temperature and can be expressed as

$$\Delta_N(T(t)) = \Delta_N \times \psi_{GW}(T(t)) \qquad [2ii]$$

and

$$\Delta_A(T(t)) = \Delta_A \times \psi_{GW}(T(t)) \qquad [2iii]$$

Incorporating variable longevity in the model requires using the time-varying form of the distributed maturation time model (Vansickle 1977).

The mortality rate ($\mu_{GW}(T)$) of adults d^{-1} at temperature T was also estimated from Son et al. (2009) (equation 3).
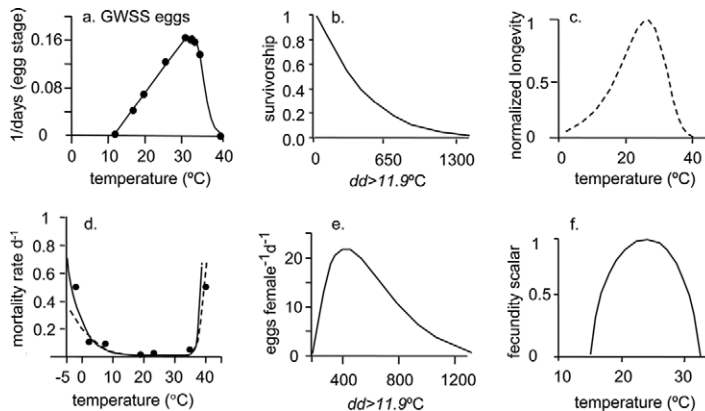

Fig. 2. The thermal biology of glassy-winged sharpshooter: (a) the developmental rate of eggs on temperature (Al-Wahaibi and Morse 2003), (b) adult survivorship on age in dd >11.9°C at 25°C, (c) the effects of temperature on normalized adult longevity, (d) the effects of temperature on adult mortality d^{-1} (data for b, c, and d are from Son et al. 2009), (e) the age specific oviposition profile for glassy-winged sharpshooter on age in dd >11.9°C at 25°C (Sétamou and Jones 2005), and (f) the normalized effect of temperature on gross fecundity (Johnson et al. 2006).

$$0 < \mu_{GW}(T) = \frac{1}{81.75\psi_{GW}(T)} < 1 \qquad [3]$$

The mortality rate data are indicated by symbol ($\bullet$), while the dashed line is equation 3 (Fig. 2d). Adults do not feed in the range 0°C< T < 11.9°C and the mortality rate is ≈0.1 d^{-1}. At $T < 0$°C and $T > 40$°C, adults survive less than the sampling interval of a day, and hence it is not surprisingly the data for $T < 0$°C are underestimated by the fitted function. A better fit for $\mu_{GW}(T)$ at low temperatures (the solid line, Fig. 2d) was obtained by adjusting the fitting parameters in equation 2i (i.e., $\rho_1 = 4.49$ and $\rho_2 = 6.049$).

Reproduction in glassy-winged sharpshooter. Sétamou and Jones (2005) reported a sex ratio of 1:1 and an average fecundity of 194 eggs/♀ at 27°C when reared on cowpea. However, Leopold et al. (2004) reported a range of 500-1100 eggs/♀, and hence we adopted a more realistic mean value of 800. To capture this biology, we used the age-specific (x) oviposition profile from Sétamou and Jones (2005) but scaled it four-fold, and fit the function proposed by Bieri et al. (1983) (equation 4i). The preoviposition period is 216 dd$_{>11.9°C}$, after which $f_{GW}(x)$ increases linearly to 22.7 eggs d^{-1} at age $x = 374.2$ dd$_{>11.9°C}$, and then declines slowly to zero (Fig. 2e).

$$f_{GW}(x) = \frac{0.167x}{1.0029^x} \qquad [4i]$$

We could add stochasticity to the model to accommodate the observed range of fecundities, but little additional clarity would accrue. Reproduction occurs in the range 13.9–32.5°C (Johnson et al. 2006), and a normalized symmetrical scalar function ($0 < \phi_{GW,ovip}(T) \leq 1$, equation 4ii) with a maximum at 23.2°C was assumed (Fig. 2f, see Gutierrez 1992, 1996).

$$0 \leq \phi_{GW,ovip}(T) = 1 - \left[\frac{T - 13.9 - 23.2}{23.2}\right]^2 \leq 1$$
$$[4ii]$$

The combined effects of age ($f_{GW}(x)$) and temperature ($\phi_{GW,ovip}(T)$) on per capita reproduction are captured by equation 4iii.

$$E_{GW}(x,T) = \phi_{GW,ovip}(T) \times f_{GW}(x) \qquad [4iii]$$

The Egg Parasitoids. Several solitary mymarid endoparasitoids attack glassy-winged sharpshooter eggs in the SE United States and NE Mexico (Triapitsyn and Phillips 2000). One of these, GA, was accidentally introduced to California (Sorensen and Gill 1996, Vickerman et al., 2004), while GT was actively introduced in 2000 (Pilkington et al. 2005). Data on both parasitoids (Pilkington and Hoddle 2006a, 2007a, Irvin and Hoddle 2007), and additional data for GA (Chen et al. 2006a, 2006b) were used to parameterize the parasitoid models.

Developmental rates. Data on the rate of development of the egg-pupal period on temperature for GA and GT are illustrated in Figs. 3a and b. Using the form of equation 1, we estimate the lower and upper ther-
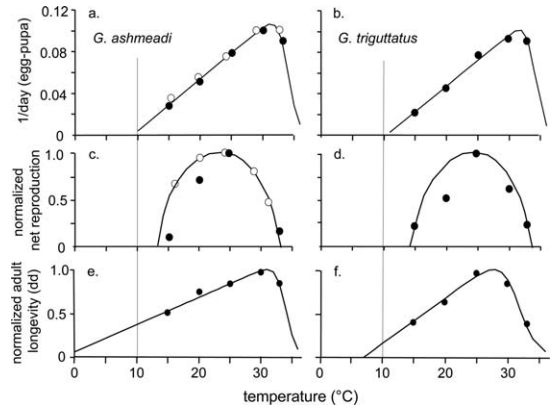

Fig. 3. The thermal biology of two-egg parasitoids of glassy-winged sharpshooter: GA (a, c, e) and GT (b, d, f): (a, b) rates of development, (c, d) normalized eggs/female, and (e, f) normalized mean adult female longevity (data from Pilkington and Hoddle (2006a, 2007a; symbol $\bullet$) and Chen et al. (2006b; symbol $\bigcirc$)).

mal thresholds for GA (9.25°C and 33.85°C), and GT (10.5°C and 34.1°C) (equation 5i, 5ii).

$$R_{GA}(T) = \frac{0.005(T - 9.25)}{1 + 4.5^{T-33.85}} \qquad [5i]$$

$$R_{GT}(T) = \frac{0.005(T - 10.5)}{1 + 4^{T-34.1}} \qquad [5ii]$$

The lower and upper thresholds for glassy-winged sharpshooter are ≈2.65 and 1.9°C higher than for GA, and 1.4 and 1.65°C higher than for GT (Fig. 2a vs. Figs. 3a and b). The mean egg-pupal (subscript I) and adult (A) developmental times for the two parasitoids in degree-days above their respective threshold are $\Delta_{I,GA} = 198dd_{>9.25°C}$, $\Delta_{A,GA} = 241dd_{>9.25°C}$, and $\Delta_{I,GT} = 204dd_{>10.5°C}$ and $\Delta_{A,GT} = 222dd_{>10.5°C}$.

Reproduction. Estimates of net parasitoid reproductive rates vary among authors, but the underlying normalized patterns are similar (Figs. 3c and d). The preoviposition period of both parasitoids is less than a day, and the per capita age-specific fecundity profiles ($f_p(x)$) for each parasitoid (subscript $p = GA, GT$) declines on age (x) at rates $r_{GA} = 0.0161, r_{GT} = 0.0273$ (equation 6i).

$$f_p(x, T = 27°C) = 110e^{-r_p x} \qquad [6i]$$

As for glassy-winged sharpshooter, the effects of temperature on the fecundity for each parasitoid (Figs. 3c and d) were captured by scalar functions ($0 \leq \phi_{ovip,p}(T) \leq 1$, equation 6ii, 6iii).

$$\phi_{ovip,GA}(T) = 1 - \left[\frac{T - 12.5 - 23.5}{23.5}\right]^2 \qquad [6ii]$$

$$\phi_{ovip,GT}(T) = 1 - \left[\frac{T - 14.5 - 24.25}{24.25}\right]^2$$
$$[6iii]$$

Ignoring species subscripts, the combined effects of $f_p(x)$ and $\phi_{ovip,p}(T)$ on age-specific per capita fecundity $(F(x,T))$ are captured by equation 6iv.

$$F_p(x,T) = \phi_{ovip,p}(T) \times 110e^{-r_p x} \qquad [6iv]$$

Realized fecundity also varies because of the effects of temperature on adult longevity (Fig. 3e and f) (Pilkington and Hoddle 2006a, 2007a), and competition among females and feeding (Irvin and Hoddle 2007, 2009; Irvin et al. 2007). Only the effects of temperature and competition are included in the model.

Adult longevity. The patterns of normalized average adult longevity on temperature (ψ_{GA} and ψ_{GT}, Figs. 3e and f) are similar to those for the developmental rates (equation 1, and hence the same function was used).

$$\psi_{GA}(T) = \frac{0.0317 \cdot (T + 2)}{1 + 3.5^{T-34}} \qquad [7i]$$

$$\psi_{GT}(T) = \frac{0.0518 \cdot (T - 7)}{1 + 2^{T-31.5}} \qquad [7ii]$$

The data extrapolated to zero, suggest that GA is more cold and heat tolerant than GT, and fitted equations 7i, ii are used to scale the maximum average adult longevity ($\Delta_{A,GA}$, $\Delta_{A,GT}$) for the effects of daily temperature (equation 8i, ii).

$$\Delta_{A,GA}(T(t)) = \Delta_{A,GA}\psi_{GA}(T(t)) \qquad [8i]$$

$$\Delta_{A,GT}(T(t)) = \Delta_{A,GT}\psi_{GT}(T(t)) \qquad [8ii]$$

As with glassy-winged sharpshooter, time varying changes in parasitoid longevity have demographic consequences that require the time-varying form of the distributed maturation-time model (Vansickle 1977).

Inter-specific competition. Irvin and Hoddle (2005) and Irvin et al. (2006) found that GA parasitized 45% more eggs of age 1–6 d than did GT, and in competition studies, overall parasitism by GA was up to 76.0% higher. Exposing both parasitoids simultaneously to high egg densities for 24 h resulted in 23% higher parasitism by GA, while parasitism rates were the same when low egg densities were exposed for 1 h. Neither parasitoid distinguishes between parasitized and unparasitized eggs.

A type III functional response model (Gutierrez and Baumgärtner 1984, Gutierrez 1996), that incorporates competition in the exponent, was used to estimate the total number of host eggs attacked (Na) because of the simultaneous action of both parasitoids (equation 9).

$$Na_{GA,GT} = (D_{GA}P_{GA} + D_{GT}P_{GT})$$
$$\left[1 - \exp\left(\frac{-(\alpha_{GA} + \alpha_{GT})H}{D_{GA}P_{GA} + D_{GT}P_{GT}} \right) \right] \quad [9]$$

Ignoring age structure for clarity of presentation, P_{GA} and P_{GT} are female parasitoid densities, D_{GA} and D_{GT} are the per capita demands for hosts (equation 6iv), H is the density of unparasitized plus parasitized eggs, and α_{GA} and α_{GT} are search functions (e.g., $0 < \alpha = s_o(1 - e^{-sP}) < s_o$ with $s_o = 0.6$, and pa-

rameters $s_{GA} = 0.025$ and $s_{GT} = 0.0125$ that reflect differences in search efficiency ($\alpha_{GA} > \alpha_{GT}$).

Na is first corrected for the proportion of previously attacked eggs, and the new attacks are distributed to each parasitoid species in proportion to their demand corrected for their search efficiency. In cases of super and multiple-parasitism, the oldest supernumerary is assumed to survive.

Weather Data. We assume nonlimiting water (irrigation) and nutrients for grape, and hence only daily maximum and minimum temperatures (°C), and solar radiation (cal cm^{-2} d^{-1}) were used as inputs for the plant model. Daily rainfall (mm), daily runs of wind (km d^{-1}) and relative humidity were also available, and could be used to run a water balance model (Ritchie 1972) for site-specific applications. However, soil moisture holding characteristics were not available at the scale of our study. Maximum and minimum temperatures were the inputs for the insect models. The term weather will refer only to these variables. Weather data from 108 locations in California for the period 1995–2006 (http://www.ipm. ucdavis.edu/) were used to run the system model. The few missing weather records at each location were estimated by linear interpolation within the data or by substituting values from a near by location.

Global climate models predict California will become warmer (1.8–3°C or more), but not drier, as precipitation as rain rather than snowfall will occur at higher elevations (http://meteora.ucsd.edu/cap/pdffiles/CA climate Scenarios.pdf). A full study of climate change effects using climate model data is beyond the scope of this study, and hence we examine only the hypothetical effects of 2° and 3°C increases in daily average temperature on potential glassy-winged sharpshooter distribution and relative abundance.

Simulation and GIS. The system model is modular, and Boolean variables in a setup file were used to determine the combinations of species in the different runs. Batch files were used to run the model across locations for the period of available weather data. The same initial population densities and other conditions were assumed at all locations (Table 1). Many of the initial field studies on glassy-winged sharpshooter occurred at Temecula, CA, and hence detailed simulation results for this location are presented to illustrate system dynamics. The system model was coded in Borland Delphi Pascal.

The geo-referenced simulation data were written to files by year, and the data were mapped for elevations below 750 m using the open source Geographic Resources Analysis Support System (GRASS) GIS software (GRASS Development Team, 2010). Inverse distance weighting interpolation of the data using the v.surf.idw GRASS module was used in mapping. The patterns in the maps reflect not only the site-specific effects of weather on the dynamics, but also the location and distances between weather stations. The system was assumed equilibrating to local conditions during 1995, and hence the simulation data for this year were not included in the summary analyses. We
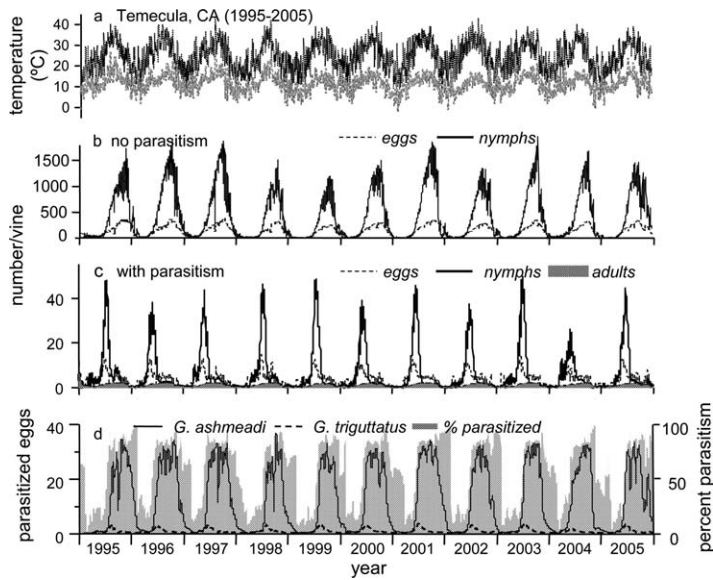
Fig. 4. The simulated dynamics of glassy-winged sharpshooter and two-egg parasitoids at Temecula, CA, during 1995 through 2005: (a) daily maximum and minimum temperatures (°C), (b) glassy-winged sharpshooter egg and nymph densities before biological control, (c) unparasitized eggs, and nymphs and adults densities after the introduction of the two-egg parasitoids, and (d) glassy-winged sharpshooter eggs parasitized by *G. ashmeadi* (——) and by *G. triguttatus* (- - -) with the shaded area being the percentage of eggs parasitized by both parasitoids.

caution that the predicted densities are indices of relative favorability.

Multiple regression across all years and locations was used to summarize the simulated effects on $\log_{10}$ total new glassy-winged sharpshooter adults y^{-1} of the two parasitoids, and season long cumulative $dda_{>11.9°C}$ and $ddb_{<11.9°C}$. The parasitoids were included in the regression model as presence-absence dummy variables (0, 1). All four combinations of parasitoids including the null set were examined. Only independent variables and interactions with slopes significantly different from zero ($P < 0.05$) were retained in the model. Marginal analysis of the regression model ($\partial y / \partial x_i$) was used to estimate the average magnitude and direction of factors affecting glassy-winged sharpshooter abundance.

Results

System dynamics at Temecula, CA. Glassy-winged sharpshooter densities and dynamics vary greatly across years and locations in California. We selected Temecula in southern California, where heavy infestations of glassy-winged sharpshooter occurred, to illustrate the richness of the system dynamics (Fig. 4, see Fig. 5c). The tick-marks on the x-axis indicating 1 January are reference points to help the reader visualize seasonality. Maximum and minimum temperatures for the 10-year period are shown in Fig. 4a.

In the absence of the parasitoids, simulated glassy-winged sharpshooter populations cycle and reach levels of 1,200–1,600 nymphs per vine during summer. Populations decline with cooling fall-winter temperatures that affect reproduction and survival (Fig. 4b).

The peak densities are similar to those recorded in the field before biological control (M. Hoddle, unpublished data).

With the addition of the parasitoids, glassy-winged sharpshooter levels decline 20–30 fold (Fig. 4c) with the contribution of GA being roughly 10-fold greater than that of GT (Fig. 4d). The combined percent parasitism of eggs reaches 80–90% during midsummer and fall, and accords well with field data showing that the majority of egg masses are attacked (Krugner et al.
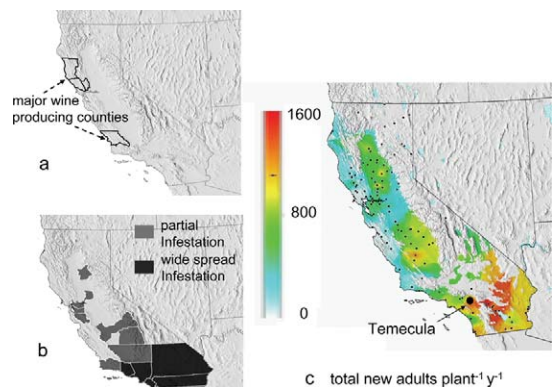

Fig. 5. Distribution of wine grape and glassy-winged sharpshooter in California: (a) the major wine grape areas, (b) the observed distribution of glassy-winged sharpshooter (Pilkington and Hoddle 2007a, 2007b), and (c) the predicted distribution of mean glassy-winged sharpshooter new adults $plant^{-1}$ y^{-1} in the absence of biological control. Temecula, CA (●) is indicated in Fig. 5c.
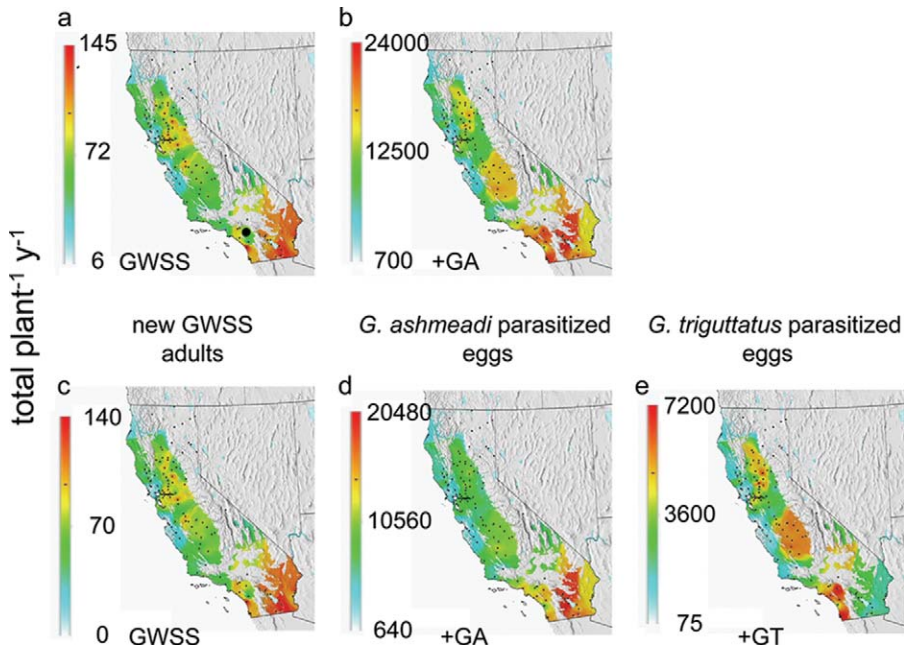
Fig. 6. GIS maps of simulated cumulative glassy-winged sharpshooter new adult densities and cumulative eggs parasitized by the two-egg parasitiods: (a) glassy-winged sharpshooter regulated by (b) GA, and (c) glassy-winged sharpshooter regulated by both (d) GA and (e) GT. Densities of the three species are average season long totals for years 1996–2005. Temecula, CA (●) is indicated in Fig. 6a.

2009). The high initial field densities of glassy-winged sharpshooter required 3 yr to suppress to levels now observed in the field. The delay in control was likely because of the outward dispersal of adult parasitoids, and the immigration of glassy-winged sharpshooter adults from surrounding high-density populations. To model these dynamics would require a meta-population model (see Gutierrez et al. 1999) of the spatial and temporal dispersal dynamics of all of the species (Park et al. 2006). The data for this are not available.

Regional Analysis. The regional analysis has two parts: (1) mapping the summary variable for glassy-winged sharpshooter density before and after biological control by egg parasitoids across California, and (2) a multiple regression or marginal analysis of the simulation data.

Glassy-winged sharpshooter before biological control. The major wine grape regions in California are shown in Fig. 5a, while the recorded distribution of glassy-winged sharpshooter is illustrated in Fig. 5b (see Pilkington and Hoddle 2007a, b). In the absence of biological control, the predicted distribution of glassy-winged sharpshooter is similar to its recorded distribution in California (Fig. 5b vs. 5c), with the major wine producing areas of northern and central California predicted to be largely unsuitable (Fig. 5a vs. 5c). The highest mean densities of glassy-winged sharpshooter adults are predicted in desert areas and the mild coastal region of southern California, with lower densities predicted in the southern and northern reaches of the Great Central Valley (Fig. 5c). The coastal and near coastal regions of northern California

are predicted to have relatively low glassy-winged sharpshooter populations.

Glassy-Winged Sharpshooter after biological control. The effects of the two-egg parasitoids on the simulated distribution and abundance of glassy-winged sharpshooter are illustrated in Fig. 6. Note that the columns in the figure indicate species and the rows species combinations. The addition of GA to the model does not change the distribution of glassy-winged sharpshooter, but does cause a 90% or more decline in new adult glassy-winged sharpshooter densities everywhere including the hot desert valleys of southern California (Fig. 5c vs. 6a). GA populations (e.g., cumulative parasitized eggs) are predicted highest in southern California with moderate levels in the southern and northern Central Valley (Fig. 6b).

Adding GT (Fig. 6e) to the interaction of glassy-winged sharpshooter and GA appears to add little to the control of glassy-winged sharpshooter (Fig. 6a vs. 6c), but it does suggest competition between the two parasitoids in most regions that causes a decline of ≈15% in GA densities across the state (Fig. 6d vs. 6b). GT is predicted rare in the hot desert regions of southern California, and is approximately ⅓ the density of GA elsewhere (Fig. 6d vs. 6e). These differences are because of the fact that GA has a higher search rate (equation 5), is more cold and heat tolerant (Fig. 3e vs. 3f), and is less aggressive with conspecific females than GT (Irvin and Hoddle 2005, Irvin et al. 2006, N. Irvin, unpublished). In the laboratory, some of these differences resulted in GA producing up to 64% more progeny than GT (Irvin and Hoddle 2005).

Table 2. Multiple regression analysis of the glassy-winged sharpshooter simulation data across locations and years

Variable	Mean	Standard deviation	Correlation x vs y	Regression coefficient	Std. error of reg. coef.	t-value
dda	1696	562.1	0.532	0.0028	0.00008	33.27
ddb	486.6	360.2	−0.385	−0.00073	0.00013	−5.59
GA^+	0.539	0.499	−0.424	−3.787	0.097	−38.92
GT^+	0.454	0.498	−0.210	−2.430	0.108	−22.49
$GA^+ \times GT^+$	0.270	0.444	−0.235	2.463	0.146	16.89
Dependent variable						
$\log_{10} A_{new}$	2.192	3.241				

Multiple regression and marginal analysis. The simulation data for $\log_{10}$ new glassy-winged sharpshooter adults ($\log_{10} A_{new}$) on presence-absence dummy variables (0, 1) for the parasitoids (GA^+ and GT^+), and season long cumulative $dda_{>11.9°C}$ and $ddb_{<11.9°C}$ across all years and locations are summarized by equation 10 and in Table 2. The goal of the analysis is heuristic, to assess the relative impact of the parasitoids, and not prediction as measured by R^2.

$$\log_{10}A_{new} = 0.324 + 0.0028dda_{>11.9°C}$$
$$- 0.00073ddb_{<11.9°C} - 3.787GA^+ - 2.430GT^+$$
$$+ 2.463GA^+ \times GT^+$$
$$R^2 = 0.532, \ df = 3802, \ F = 866.57 \quad [10]$$

Given the average effects of the other variables and using mean values for the independent variables, the effects of $dda_{>11.9°C}$ on $\log_{10}A_{new}$ is large and positive (e.g., $0.0028 \times 1696 = 4.75$), while $ddb_{<11.9°C}$ has a smaller decreasing effect ($-0.000727 \times 486.6 = -0.35$). The effects of GA^+ (-3.79 by $0.54 = -2.04$) and GT^+ ($-2.43 \times 0.45 = -1.10$) are negative, but the interaction $GA^+ \times GT^+$ is positive ($2.463 \times 0.27 = 0.665$) suggesting competition.

Taking the antilog of equation 10 converts the components to yearly population growth and survivorship rates. Average A_{new} survivorship because of GA^+ alone is $10^{-2.04} = 0.0091$, $10^{-1.1} = 0.0794$ for GT^+ alone, and $10^{-2.04-1.1+0.665} = 0.0034$ with both parasitoids. GT^+ increases average A_{new} mortality only slightly over GA^+ alone (e.g., $(1-0.0034) - (1-0.0091) = 0.0058$). The value 0.0058 is a measure of GT^+ average indispensable mortality, with still smaller values expected in hotter areas of the state. For example, the predicted statewide average density of GA is three-fold that of GT, but GA densities are eight-fold greater in the hot desert region (Fig. 6d vs. 6e).

The Distribution of the Pathogen X. fastidiosa. To include the full dynamics of Pierce's disease in the model would require the development of a metapopulation model composed of populations of plants with the movement of vectors and disease between them (e.g., Gutierrez et al. 1999). This is clearly beyond the scope of this study. Important insights, however, can be gained from a simpler analysis. For example, plotting the in vitro growth rate (R_{Xf}) for *X. fastidiosa* on temperature yields a familiar relationship (equation 11 with lower (12.50°C) and upper (32.25°C) thresholds (see Fig. 7a).

$$R_{Xf} = \frac{0.00865 \cdot (T - 12.50)}{1 + 2.75^{T-32.25}} \quad [11]$$

The range of favorable temperatures for the pathogen is narrower (solid line, Fig. 7a) than that of glassy-winged sharpshooter which is 11.90°C to 35.75°C (see Fig. 2a).

A more meaningful metric for disease favorability is the concave normalized growth index (*PDI*, see equation 4.ii) that captures the thermal limits and the optimum at the midpoint of the favorable range (dashed line, Fig. 7a). Mapping the 10-yr average *PDI* (Fig. 7b) shows that the area most favorable for the pathogen is similar to that for glassy-winged sharpshooter in southern California, but it is dissimilar in northern area where cold limits the pathogen (Feil and Purcell 2001; Purcell 1980, 1997) more than it does glassy-winged sharpshooter (Fig. 5c vs. 7b).

Daugherty et al. (2009) found that inoculation efficiency of glassy-winged sharpshooter is positively related to temperature and the number of infectious vectors. We can capture this notion as the product of *PDI* (Fig. 7b) and an index of normalized total new adults given the action of natural enemies (*GWI*, data from Fig. 6c). The interaction *PDI* × *GWI* predicts a further restriction of the geographic range for disease favorability in southern California because of the action of the egg parasitoids (Fig. 7b vs. 7c).
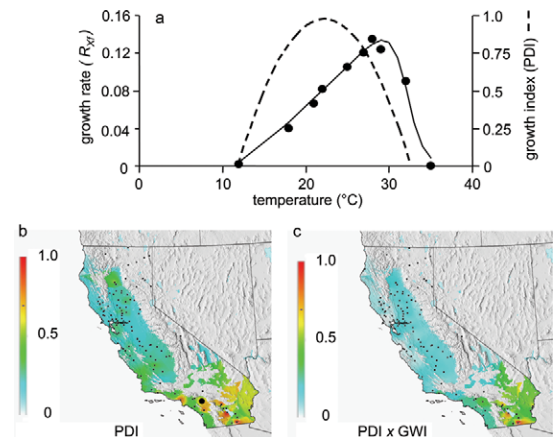

Fig. 7. The pathogen *X. fastidiosa:* (a) in vitro growth rate d^{-1} (R_{Xf}, —) and normalized growth rate index (*PDI*, —-) on temperature (Feil and Purcell 2001), and the distribution of (b) mean *PDI*, and (c) mean *PDI* × *GWI* across California (see text for definitions of *PDI* and *GWI*).

Discussion

Calls for holistic analyses of agricultural and natural systems are often made (e.g., Sutherst and Bourne 2009), but rarely does this occur. However, holistic approaches are needed for predicting the geographic distribution and relative abundance of invasive species and their control across ecological zones (e.g., Mills and Getz 1996). The most common methods used to assess such problems fall under the ambit of ENMs, but more holistic PBDMs, as used here, are also beginning to appear (see below). ENMs are commonly formulated using weather and other abiotic factors from the native geographic range of the invasive species, and are then used to estimate the potential distribution in extant and in new areas. ENMs may be statistical (see Estrada-Peña 2008, Mitikka et al. 2008)); applications based on artificial intelligence concepts (Phillips et al. 2006); and physiological index models (e.g., Fitzpatrick and Nix 1968, Gutierrez et al. 1974, Sutherst and Maywald 1985). ENMs based on these techniques assume the current species distribution is the best indicator of its climatic requirements, the distribution is in equilibrium with current climate, and climate niche conservatism is maintained in both space and time (Beaumont et al. 2009). Other factors may adversely affect the predictions of ENMs: trophic interactions, the use of average weather data that may miss important and frequent short-term weather events, the assumed native range may be in error leading to over or under estimates of the distribution (Davis et al. 1998), and different ENM approaches may give different predictions. Roura-Pascual et al. (2009) compared five ENM methods to predict the potential distribution of Argentine ants in the Iberian Peninsula, and found differences in geographic predictions and in the ability to identify areas of uncertainty regarding the ant's invasive potential. Hickler et al. (2009) further cautioned that process-based representations of water balance in terrestrial ecosystems should be included in ENMs, and we might add, in PBDMs. A mechanistic soil water-balance model to characterize water effects on plant growth and fruiting proved critical in a PBDM analysis of the attempted biological control of the invasive annual yellow starthistle (*Centaurea solstitialis*) by seed-head feeding herbivores (Gutierrez et al. 2005). Despite shortcomings, Thuiller et al. (2005) posits that ENMs may provide powerful, unbiased first-steps for screening the potential range of invasive species in new areas.

ENMs and life-table statistics have been used to examine the geographic distribution and invasiveness of the polyphagous glassy-winged sharpshooter, the distribution of its two-egg parasitoids (GA and GT), and the potential distribution of the PD pathogen *X. fastidiosa.* Hoddle (2004) used the physiological-index CLIMEX algorithm (Sutherst et al. 1991) to estimate the geographic limits of glassy-winged sharpshooter and the pathogen. Unfortunately, the coarse grain predictions of the CLIMEX model proved difficult to compare with the fine grain predictions of our PBDM (see below).

Pilkington and Hoddle (2006b, 2007b) used long-term average daily temperatures to estimate the number of generations, and the net reproductive rates (R_o) of GA and GT in California. Using R_o as a metric, the predicted area of highest favorability for both parasitoids was the hot desert valleys of southern California, with the distribution of GA being much wider than for GT. The predictions for GA but not GT are similar to those of our PBDM system (see below).

A PBDM System for Grape/Glassy-Winged Sharpshooter/Parasitoids. We propose that some of the deficiencies of ENM approaches may be overcome using the PBDM approach. Instead of starting from the assumed geographic distribution of a species, a PBDM system captures the weather-driven biology of the interacting species, and uses it to map the dynamics (niche) of the species in time and space. A PBDM system can incorporate the bottom-up effects of plant growth and development, the top-down action of natural enemies, and important physiology and behavior of all of the species (e.g., Gutierrez et al. 2005, 2007, 2009, 2010; Ponti et al. 2009).

Using daily maximum and minimum temperature and solar radiation, the system model predicts that in the absence of natural enemies, the most favorable areas for glassy-winged sharpshooter are coastal and near coastal southern California, the southern desert area, and to a lesser extent, portions of the lower and upper Central Valley (Fig. 5c). The major wine growing regions of California (Fig. 5a) are predicted marginal for glassy-winged sharpshooter (Fig. 5c). In southern California, the model predicts two to three glassy-winged sharpshooter generations per season (Hummel et al. 2006) with peak glassy-winged sharpshooter populations occurring in early to midsummer (Krugner et al. 2009). The geographic distribution of glassy-winged sharpshooter in California is not affected by the two-egg parasitoids, but adult glassy-winged sharpshooter abundance is reduced >90% across the state (Fig. 5c vs. 6c). GA is the most effective parasitoid with a small average indispensable mortality of <1% contributed by GT. The potential range of the pathogen *X. fastidiosa* is considerably less than that of glassy-winged sharpshooter, but with the biological control of glassy-winged sharpshooter, the potential range of the pathogen is reduced still further to the desert regions of southern California (Fig. 7b and c).

The system model can be applied to other areas globally where glassy-winged sharpshooter may invade. For example, glassy-winged sharpshooter invaded the tropical island of Moorea and neighboring islands of French Polynesia in 1999, where its numbers exploded in response to highly favorable weather, and aided by its toxicity to native generalist predators (Suttle and Hoddle 2006). However, the introduction of GA to Moorea in 2005 led to rapid control of glassy-winged sharpshooter (Grandgirard et al. 2009). Our model, without modification, predicted these dynamics (not shown).
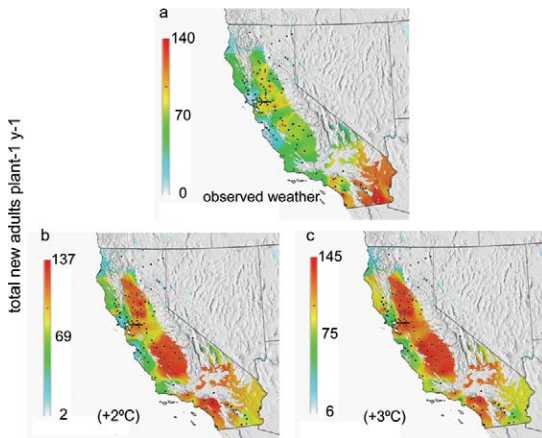
Fig. 8. Effects of observed temperatures and two warming scenarios on the average geographic distribution and abundance of total new glassy-winged sharpshooter adults plant^{-1} y^{-1} given the action of two-egg parasitoids (GA and GT): (a) with observed temperatures; with daily average increases of (b) 2°C and (c) 3°C.

Other factors that may influence the dynamics of glassy-winged sharpshooter include the level of amino acids in host plants (Bi et al. 2005), diurnal and seasonal changes in nutrient-poor xylem (Mizell et al. 2008), and plant water stress (Krugner et al. 2009). We were unable to include these factors in the model, but suspect that their omission would not qualitatively affect our conclusions.

Effects of warming temperatures. Temperatures are expected to increase in California ≈1.8–3°C, but a full study of the effects of climate warming on the grape/glassy-winged sharpshooter system is beyond the scope of this study (see Gutierrez et al. 2006). Here we pose a simpler hypothetical question: how would warming temperatures in glassy-winged sharpshooter' current distribution affect its abundance?

The model predicts that increasing average daily temperatures 2°C and 3°C would increase glassy-winged sharpshooter abundance throughout much of California, except in the southern deserts where increased summer temperatures would approach its upper thresholds for survival and reproduction (Fig. 8a vs. Figures 8b and c). Glassy-winged sharpshooter and the pathogen are predicted to increase in important agricultural areas of California, especially in the Central Valley. Control of glassy-winged sharpshooter by the egg parasitoids would not be affected.

Comments on invasive species policy. Without benefit of sound analysis, new invasive species tend to be approached in a crisis mode that may result in large sums of money being spent on questionable control and eradication efforts (e.g., medfly, *Ceratitis capitata* Weidemann; Gutierrez and Ponti 2011). Glassy-winged sharpshooter is a case in point when it first invaded California. Fortunately, a successful biological control program using GA likely has helped solve the problem. However, such good results may not occur with other invasive species, and holistic ap-

proaches are needed to assess their invasive potential and geographic range. Such analyses could serve as a basis for formulating sound ecological and economic policy for containment/eradication/management efforts, and for evaluating the efficacy of control programs. This need was aptly illustrated by a prospective PBDM analysis of the exotic light brown apple moth (*Epiphyas postvittana* Walker) that was first found in coastal north-central California in 2006. The PBDM analysis showed, as observed, that the geographic range of the moth was largely near coastal, its populations were low because of good natural control, that eradication was likely unachievable, and the proposed containment strategy was unrealistic (Gutierrez et al. 2010). More recently, the European grape vine moth (*Lobesia botrana* (Den. and Schiff.)), a common pest of grape in the Mediterranean area, was discovered in 2008 in Napa County in the heart of Northern California's wine country. It has since been found in eight additional counties, some of which are in the Central Valley. A prospective PBDM analysis posits that *Lobesia* could spread statewide and beyond, eradication of the pest may not be possible, and pest management procedures may need to be developed and implemented (Gutierrez et al. submitted).

Thus, PBDMs can be used in a prospective manner to gauge the potential geographic distribution of new pests in their native areas or in newly invaded ones, and with appropriate agronomic/ecological layers, PBDMs can be used to evaluate pest impact and management options at the local and regional level. Unfortunately, sound biological data to parameterize a PBDM for a new invasive species and the weather data to drive it may not be available at the beginning of the invasion. However, given a modest scientific infrastructure and budget, the necessary data can be gathered efficiently using the model framework as a guide. In addition, climate model weather data are increasingly available, and can be used with the model to explore the effects of climate change (Gutierrez et al. 2006).

References Cited

Adlerz, W. C. 1980. Ecological observations on two leafhoppers that transmit the Pierce's disease bacteria. Proc. Fla. State Hort. Soc. 93: 115–120.

Almeida, R.P.P., and A. H. Purcell. 2003. Transmission of *Xylella fastidiosa* to grapevines by *Homalodisca coagulata* (Hemiptera: Cicadellidae). J. Econ. Entomol. 96: 264–271.

Al-Wahaibi, A. K., and J. G. Morse. 2003. Homalodisca coagulata (Hemiptera: Cicadellidae) embryonic development at constant temperatures. Fla. Entomol. 86: 477–478.

Andrewartha H. G., and L. C. Birch. 1954. The Distribution and Abundance of Animals. University of Chicago Press, Chicago.

Beaumont, L. J., R. V. Gallagher, W. Thuiller, P. O. Downey, M. R. Leishman, and L. Hughes. 2009. Different climatic envelopes among invasive populations may lead to under estimations of current and future biological invasions. Diversity Distrib. 15: 409–420.

Bi, J. L., S. J. Castle, F. J. Byrne, S. J. Tuan, and N. C. Toscano. 2005. Influence of seasonal nitrogen nutrition fluctuations in orange and lemon trees on population dynamics of the glassy-winged sharpshooter (*Homalodisca coagulata*). J. Chem. Ecol. 31: 2289–2306.

Bieri, M., J. Baumgärtner, G. Bianchi, V. Delucchi, and R. von Arx. 1983. Development and fecundity of pea aphid (*Acyrthosiphon pisum* Harris) as affected by constant temperatures and by pea varieties. Mitt. Schwei. Entomol. Ges. 56: 163–171.

Blua, M. J., R. A. Redak, D.J.W. Morgan, and H. S. Costa. 2001. Seasonal flight activity of two *Homalodisca* species (Homoptera: Cicadellidae) that spread *Xylella fastidiosa* in Southern California. J. Econ. Entomol. 94: 1506–1510.

Brière, J. F., P. Pracros, A. Y. Le Roux, and J. S. Pierre. 1999. A novel rate model of temperature-dependent development for arthropods. Environ. Entomol. 28: 22–29.

Brodbeck, B. V., P. C. Andersen, R. F. Mizell, III, and S. Oden. 2004. Comparative nutrition and developmental biology of xylem-feeding leafhoppers reared on four genotypes of *Glycine max*. Environ. Entomol. 33: 165–173.

(CDFA) California Department of Food and Agriculture. 2003. Pierce's disease program report to the legislature, May 2003. California Department of Food and Agriculture, 8–11 December, 2003, San Diego, CA.

(CDFA) California Department of Food and Agriculture. 2005. Pierce's disease control program. (http//www.cdfa.ca.gov/phpps/pdcp/index.htm).

Chen, Wen-Long, R. A. Leopold, and M. O. Harris. 2006a. Parasitism of the glassy-winged sharpshooter, Homalodisca coagulata (Homoptera: Cicadellidae): functional response and superparasitism by *Gonatocerus ashmeadi* (Hymenoptera: Mymaridae). Biol. Control. 37: 119–129.

Chen, Wen-Long, R. A. Leopold, D.J.W. Morgan, and M. O. Harris. 2006b. Development and reproduction of the egg parasitoid, Gonatocerus ashmeadi Girault (Hymenoptera: Mymaridae), as a function of temperature. Environ. Entomol. 35: 1178–1187.

Daugherty, M. P., D. Bosco, and R.P.P Almeida. 2009. Temperature mediates vector transmission efficiency: inoculum supply and plant infection dynamics. Ann. Appl. Biol. 155: 361–369.

Davis, A. J., L. S. Jenkinson, J. H. Lawton, B. Shorrocks, and S. Wood. 1998. Making mistakes when predicting shifts in species range in response to global warming. Nature. 391: 783–786.

DeBach, P., and R. A. Sundby. 1963. Competitive displacement between ecological homologues. Hilgardia. 35: 105–166.

DiCola, G., G. Gilioli, and J. Baumgärtner. 1999. Mathematical models for age-structured population dynamics, pp. 503–531. *In* C. B. Huffaker, and A. P. Gutierrez (eds.), Ecological Entomology, 2nd ed. Wiley, New York.

Estrada-Peña, A. 2008. Climate, niche, ticks, and models: what they are and how we should interpret them. Parasitol. Res. 103: 87–95.

Feil, H., and A. H. Purcell. 2001. Temperature-dependent growth and survival of *Xylella fastidiosa* in vitro and in potted grapevines. Plant Disease. 85: 1230–1234.

Fitzpatrick, E. A., and H. A. Nix. 1968. The climatic factor in Australian grasslands ecology, pp. 3–26. *In* R. M. Moore (ed.), Australian Grasslands. Australian National University Press, Canberra, ACT, Australia.

Grandgirard, J., M. S. Hoddle, J. N. Petit, J. K. Roderick, and N. Davies. 2009. Classical biological control of the glassy-winged sharpshooter, Homalodisca vitripennis, by the egg parasitoid *Gonatocerus ashmeadi* in the Society, Marquesas and Austral archipelagos of French Polynesia. Biol. Control. 48: 155–163.

GRASS Development Team. 2010. Geographic Resources Analysis Support System (GRASS) Software, Version 6.4.0. Open Source Geospatial Foundation. (http://grass.osgeo.org).

Gutierrez, A. P. 1992. The physiological basis of ratio dependent theory. Ecology. 73: 1529–1553.

Gutierrez, A. P. 1996. Applied Population Ecology: A Supply-Demand Approach. Wiley, New York.

Gutierrez, A. P., and J. U. Baumgärtner. 1984. Multitrophic level models of predator-prey-energetics: I. age specific energetics models-pea aphid *Acyrthosiphon pisum* (Harris) (Homoptera: Aphididae) as an example. Can. Entomol. 116: 924–932.

Gutierrez, A. P., K. M. Daane, L. Ponti, V. M. Walton, and C. K. Ellis. 2007. Prospective evaluation of the biological control of the vine mealybug: refuge effects. J. Appl. Ecol. 44: 1–13.

Gutierrez, A. P., N. J. Mills, and L. Ponti. 2010. Limits to the potential distribution of light brown apple moth in Arizona-California based on climate suitability and host plant availability. Biol. Invasions. 12: 3319–3331.

Gutierrez, A. P., H. A. Nix, D. E. Havenstein, and P. A. Moore. 1974. The ecology of *Aphis craccivora* Koch and Subterranean Clover Stunt Virus in south-east Australia. III. A regional perspective of the phenology and migration of the cowpea aphid. J. Appl. Ecol. 11: 21–35.

Gutierrez, A. P., M. J. Pitcairn, C. K. Ellis, N. Carruthers, and R. Ghezelbash. 2005. Evaluating biological control of yellow starthistle (*Centaurea solstitialis*) in California: a GIS based supply–demand demographic model. Biol. Control. 34: 115–131.

Gutierrez, A. P., L. Ponti, and Q. A. Cossu. 2009. Effects of climate warming on olive and olive fly (*Bactrocera oleae* (Gmelin)) in California and Italy. Climatic Change 95: 195–217.

Gutierrez, A. P., and L. Ponti. 2011. Assessing the invasive potential of the Mediterranean fruit fly in California and Italy. Biol. Invasions doi:10.1007/s10530–011-9937–6.

Gutierrez, A. P., L. Ponti, C. K. Ellis, and T. d'Oultremont. 2006. Analysis of climate effects on agricultural systems: A report to the Governor of California sponsored by the California Climate Change Center. (http://www.energy.ca.gov/2005publications/CEC-500–2005-188/CEC-500–2005-188-SF.PDF).

Gutierrez, A. P., L. Ponti, M. L. Cooper, G. Gilioli, J. Baumgärtner, and C. Duso. (submitted). Prospective analysis of the invasive potential of the European grapevine moth (*Lobesia botrana* (Den. & Schiff.)) in California. Agric. For. Entomol.

Gutierrez, A. P., D. W. Williams, and H. Kido. 1985. A model of grape growth and development: the mathematical structure and biological considerations. Crop Sci. 25: 721–728.

Gutierrez, A. P., J. S. Yaninek, P. Neuenschwander, and C. K. Ellis. 1999. A physiologically based meta-population dy-

namics: the tritrophic cassava system as a case study. Ecol. Modelling 123: 225–242.

Hickler, T., S. Fronzek, M. B. Araújo, O. Schweiger, W. Thuiller, and M. T. Sykes. 2009. An ecosystem model-based estimate of changes in water availability differs from water proxies that are commonly used in species distribution models. Global Ecol. Biogeogr. 18: 304–313.

Hoddle, M. S. 2004. The potential adventive geographic range of glassy-winged sharpshooter, Homalodisca coagulata and the grape pathogen *Xylella fastidiosa:* Implications for California and other grape growing regions of the world. Crop Prot. 23: 691–699.

Hopkins, D. L., and A. H. Purcell. 2002. Xylella fastidiosa: cause of Pierce's disease of grapevine and other emergent diseases. Plant Dis. 86: 1056–66.

Huffaker, C. B., and C. E. Kennett. 1959. A ten-year study of the vegetational changes associated with the biological control of klamath weed. J. Range Manage. 12: 69–82.

Huffaker, C. B., and C. E. Kennett. 1966. Studies of two parasites of the olive scale, Parlatoria oleae (Colvée). IV. Biological control of *Parlatoria oleae* (Colvée) through the compensatory action of two introduced parasites. Hilgardia. 37: 283–334.

Hummel, N. A., F. G. Zalom, N. C. Toscano, P. Burman, and C.Y.S. Peng. 2006. Seasonal patterns of female *Homalodisca Coagulata* (Say) (Hemiptera: Cicadellidae) reproductive physiology in Riverside, California. Environ. Entomol. 35: 901–906.

Irvin, N. A., and M. S. Hoddle. 2005. The competitive ability of three mymarid egg parasitoids (*Gonatocerus spp.*) for glassy-winged sharpshooter (*Homalodisca coagulata*) eggs. Biol. Control. 34: 204–214.

Irvin, N. A., and M. S. Hoddle. 2007. Evaluation of floral resources for enhancement of fitness of *Gonatocerus ashmeadi*, an egg parasitoid of the glassy-winged sharpshooter, *Homalodisca vitripennis.* Biol. Control. 40: 80–88.

Irvin, N. A., and M. S. Hoddle. 2009. Egg maturation, oosorption, and wing wear in *Gonatocerus ashmeadi (Hymenoptera: Mymaridae), an egg parasitoid of the glassy-winged sharpshooter, Homalodisca vitripennis* (Hemiptera: Cicadellidae). Biol. Control. 48: 125–132.

Irvin, N. A., M. S. Hoddle, and S. J. Castle. 2007. The effect of resource provisioning and sugar composition of foods on longevity of three *Gonatocerus* spp., egg parasitoids of *Homalodisca vitripennis.* Biol. Control 40: 69–79.

Irvin, N. A., M. S. Hoddle, and D.J.W. Morgan. 2006. Competition between *Gonatocerus ashmeadi* and *G. triguttatus* for glassy-winged sharpshooter (*Homalodisca coagulata*) egg masses. Biocontrol Sci. Technol. 16: 359–375.

Johnson, M., K. M. Daane, R. Groves, E. Backus, and Y. Son. 2006. Spatial population dynamics and over wintering biology of the glassy-winged sharpshooter, *Homalodisca coagulata*, in California's San Joaquin Valley, pp. 12–15. In M. A. Tariq, R. Medeiros, R. Mochel, and S. Veling (eds.), Proceedings of the Pierce's Disease Research Symposium, San Diego, CA, 27–29 November 2006. California Department of Food and Agriculture, Copeland Printing, Sacramento,

Krugner, C. A., R. L. Groves, M. W. Johnson, A. P. Flores, J. R. Hagler, and J. G. Morse. 2009. Seasonal population dynamics of *Homalodisca vitripennis* (Hemiptera: Cicadellidae) in sweet orange trees maintained under continuous deficit irrigation. J. Econ. Entomol. 102: 960–973.

Lauzière, I., and M. Sétamou. 2009. Suitability of different host plants for oviposition and development of *Homalodisca Vitripennis* (Hemiptera: Cicadellidae) and its implication on mass rearing. Ann. Entomol. Soc. Am. 102: 642–649.

Leopold, R. A., W. Chen, and G. D. Yocum. 2004. Effects of using constant temperature and cyclical stepwise-increasing temperatures on parasitized and unparasitized eggs of the glassy-winged sharpshooter during cold storage, pp. 124–127. In M. Athar Tariq, S. Oswalt, P. Blincoe, A. Ba, T. Lorick, and T. Esser (eds.), Proceedings of the Pierce's Disease Research Symposium, 7–10 December 7–10, San Diego, CA. Copeland Printing, Sacramento, CA.

Mills, N. J., and W. M. Getz. 1996. Modelling the biological control of insect pests: a review of host-parasitoid models. Ecol. Modelling. 92: 121–143.

Mitikka, V., R. K. Heikkinen, M. Luoto, M. B. Araújo, K. Saarinen, J. Pöyry, and S. Fronzek. 2008. Predicting range expansion of the map butterfly in Northern Europe using bioclimatic models. Biodivers. Conserv. 17: 623–641.

Mizell, III, R. F., C. Tipping, P. C. Andersen, B. V. Brodbeck, W. B. Hunter, and T. D. Northfield. 2008. Behavioral model for *Homalodisca vitripennis* (Hemiptera: Cicadellidae): optimization of host plant utilization and management implications. Environ. Entomol. 37: 1049–1062.

Park, Y.-L., T. M. Perring, R. Yacoub, D. W. Bartels, and D. Elms. 2006. Spatial and temporal dynamics of overwintering *Homalodisca coagulata* (Hemiptera: Cicadellidae). J. Econ. Entomol. 99: 1936–1942.

Perring, T. M., C. A. Farrar, and M. J. Blua. 2001. Proximity to citrus influences Pierce's disease in Temecula Valley vineyards. Calif. Agric. 55: 13–18.

Phillips, S. J., R. P. Anderson, and R. E. Schapire. 2006. Maximum entropy modeling of species geographic distributions. Ecol. Modelling. 190: 231–259.

Pilkington, L. J., and M. S. Hoddle. 2006a. Reproductive and developmental biology of *Gonatocerus ashmeadi* (Hymenoptera: Mymaridae), an egg parasitoid of *Homalodisca coagulata* (Hemiptera: Cicadellidae). Biol. Control. 37: 266–275.

Pilkington, L. J., and M. S. Hoddle. 2006b. Use of life table statistics and degree-day values to predict the invasion success of *Gonatocerus ashmeadi* (Hymenoptera: Mymaridae), an egg parasitoid of *Homalodisca coagulata* (Hemiptera: Cicadellidae), in California. Biol. Control. 37: 276–283.

Pilkington, L. J., and M. S. Hoddle. 2007a. Use of life tables to quantify reproductive and developmental biology of *Gonatocerus triguttatus* (Hymenoptera: Mymaridae), an egg parasitoid of *Homalodisca vitripennis* (Hemiptera: Cicadellidae). Biol. Control. 42: 1–8.

Pilkington, L. J., and M. S. Hoddle. 2007b. Predictions of invasion success of *Gonatocerus triguttatus* (Hymenoptera: Mymaridae), an egg parasitoid of *Homalodisca vitripennis* (Hemiptera: Cicadellidae), in California using life table statistics and degree–day values. Biol. Control. 42: 9–15.

Pilkington, L. J., N. A. Irvin, E. A. Boyd, M. S. Hoddle, S. V. Triapitsyn, B. G. Carey, W. A. Jones, and D.J.W. Morgan. 2005. Introduced parasitic wasps could control glassy-winged sharpshooter. Calif. Agric. 59: 223–228.

Pimentel, D., L. Lach, R. Zuniga, and D. Morrison. 2000. Environmental and economic costs of non-indigenous species in the United States. BioScience 50: 53–65.

Ponti, L., Q. A. Cossu, and A. P. Gutierrez. 2009. Climate warming effects on the *Olea europaea–Bactrocera oleae* system in Mediterranean islands: Sardinia as an example. Global Change Biol. 15: 2874–2884.

Purcell, A. H. 1980. Environmental therapy for Pierce's disease of grapevines. Plant Dis. 64: 388–390.

Purcell, A. H. 1997. Xylella fastidiosa, a regional problem or global threat? J. Plant Pathol. 79: 99–105.

Purcell, A. H., and S. R. Saunders. 1999. Glassy-winged sharpshooters expected to increase plant disease. Calif. Agric. 53: 26–27.

Quezada, J. R., and P. DeBach. 1973. Bioecological and population studies of the cottony scale, Icerya purchasi Mask, and its natural enemies, *Rodolia cardinalis* Mul. and *Cryptochaetum iceryae* Wil., in southern California. Hilgardia. 41: 631–688.

Redak, R., A. H. Purcell, J.R.S. Lopes, M. J. Blua, R. F. Mizell, III, and P. C. Andersen. 2004. The biology of xylem fluid–feeding insect vectors of *Xylella fastidiosa* and their relation to disease epidemiology. Annu. Rev. Entomol. 49: 243–270.

Regev, U., A. P. Gutierrez, S. J. Schreiber, and D. Zilberman. 1998. Biological and economic foundations of renewable resource exploitation. Ecol. Econ. 26: 227–242.

Ritchie, J. T. 1972. Model for predicting evaporation from a row crop with incomplete cover. Water Resour. Res. 8: 1204–1213.

Rochat, J., and A. P. Gutierrez. 2001. Weather mediated regulation of olive scale by two parasitoids. J. Anim. Ecol. 70: 476–490.

Roura-Pascual, N., L. Brotons, P. A. Townsend, and W. Thuiller. 2009. Consensual predictions of potential distributional areas for invasive species: a case study of Argentine ants in the Iberian Peninsula. Biol. Invasions. 11: 1017–1031.

Sétamou, M., and W. A. Jones. 2005. Biology and biometry of sharpshooter *Homalodisca Coagulate* (Homoptera: Cicadellidae) reared on cowpea. Ann. Entomol. Soc. Am. 98: 322–328.

Son, Y., R. L. Groves, K. M. Daane, D.J.W Morgan, and M. W. Johnson. 2009. Influences of temperature on *Homalodisca vitripennis* (Hemiptera: Cicadellidae) survival under various feeding conditions. Environ. Entomol. 38: 1485–1495.

Sorensen, J. T., and R. J. Gill. 1996. A range extension of *Homalodisca coagulata* (Say) (Hemiptera: Clypeorrhyncha: Cicadellidae) to southern California. Pan-Pac. Entomol. 72: 160–161.

Sutherst, R. W., and A. S. Bourne. 2009. Modelling non-equilibrium distributions of invasive species: a tale of two modelling paradigms. Biol. Invasions. 11: 1231–1237.

Sutherst, R. W., and G. F. Maywald. 1985. A computerized system for matching climates in ecology. Agric Ecosyst Environ. 13: 281–299.

Sutherst, R. W., G. F. Maywald, and W. Bottomly. 1991. From CLIMEX to PESKY, a generic expert system for risk assessment. EPPO Bulletin 21: 595–608.

Suttle, K. B., and M. S. Hoddle. 2006. Engineering enemy-free space: an invasive pest that kills its predators. Biol. Invasions. 8: 639–649.

Thuiller, W., D. M. Richardson, P. Pysek, G. F. Midgley, G. O. Hughes, and M. Rouget. 2005. Niche-based modelling as a tool for predicting the risk of alien plant invasions at a global scale. Global Change Biol. 11: 2234–2250.

Triapitsyn, S. V., and P. A. Phillips. 2000. First record of *Gonatocerus triguttatus* (Hymenoptera: Mymaridae) from eggs of *Homalodisca coagulata* (Homoptera: Cicadellidae) with notes on the distribution of the host. Fla. Entomol. 83: 200–203.

Turner, W. F., and H. N. Pollard. 1959. Life histories and behavior of five insect vectors of phony peach disease. U.S. Dep. Agric. Tech. Bull. 1188: 28.

Vansickle, J. 1977. Attrition in distributed delay models. IEEE Trans. Syst. Manage. Cyber. 7: 635–638.

Vickerman, D. B., M. S. Hoddle, S. Triapitsyn, and R. Stouthamer. 2004. Species identity of geographically distinct populations of the glassy-winged sharpshooter parasitoid *Gonatocerus ashmeadi*: morphology, DNA sequences, and reproductive compatibility. Biol. Control. 31: 338–345.

Walther, G. R. 2002. Ecological responses to recent climate change. Nature 416: 389–395.

Wellington, W. G., D. L. Johnson, and D. J. Lactin. 1999. Weather and insects, pp. 313–353. *In* C. B. Huffaker, and A. P. Gutierrez (eds.), Ecological Entomology, 2nd ed. Wiley, New York.

Wells, J. M., B. C. Raju, H. Y. Hung, W. G. Weisburg, L. M. Paul, and D. J. Brenner. 1987. *Xylella fastidiosa* gen. nov., sp. nov: gram-negative, xylem-limited, fastidious plant bacteria related to *Xanthomonas spp.* Int. J. Syst. Bacteriol. 37: 136–143.

Wermelinger, B., J. Baumgärtner, and A. P. Gutierrez. 1991. A demographic model of assimilation and allocation of carbon and nitrogen in grapevines. Ecol. Modelling 53: 1–26.

Appendix: Brief Overview of the Distributed-Maturation-Time Dynamics Model

The physiologically based demographic model (PBDM) approach builds on the idea that all organisms are consumers and all have similar problems of resource acquisition (inputs) and allocation (outputs) (Gutierrez 1992). This notion allows the use of the same resource acquisition model and birth-death dynamics models to describe all trophic levels including the economic one (Regev et al. 1998). For consumers such as grape and glassy-winged sharpshooter, the model for per capita resource acquisition (i.e., the *supply, S*) is search driven by total consumer demands (*D*) in priority order for egestion, conversion costs, respiration (i.e., the Q_{10} rule in ectotherms), and reproduction, growth, and reserves. The ratio $0 \leq S/D < 1$ is always less than unity because of imperfect consumer search, and is used in the model to scale maximal vital rates of species. Parasitoid seeks hosts (e.g., eggs) as outlined in the text.

The Erlang distributed-maturation-time demographic model is widely used to simulate the age structured population dynamics of species. Details concerning the time invariant and time varying models are found in Vansickle (1977) and DiCola et al. (1999, pp. 523–524). The general form of the time invariant model for the *i*th age class of a population is as follows.

$$\frac{dN_i}{dt} = \frac{k\Delta_x}{\Delta}[N_{i-1}(t) - N_i(t)] - \mu_i(t)\,N_i(t)$$

$$[A1]$$

N_i is the density (mass or numbers) of the *i*th age class,
dt is a change in time (e.g., a day),
k is the number of age classes,
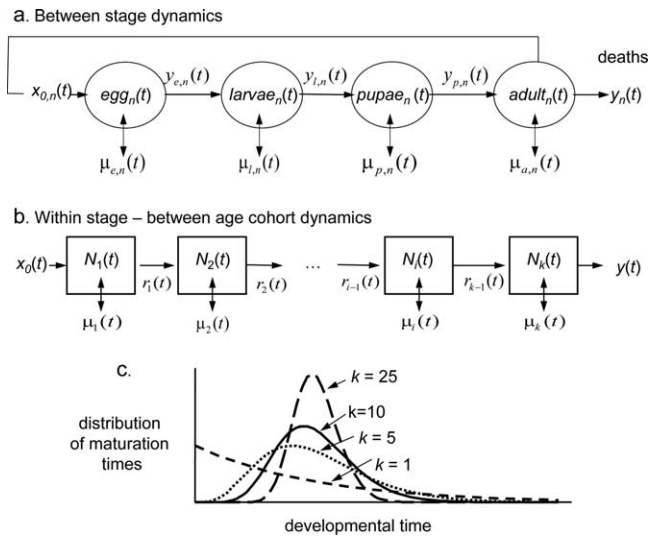Δ is the expected mean developmental time,

Fig. A1. The distributed maturation time model: (a) flow between life stages for species n, (b) flow between age cohorts within a life stage, and (c) distribution of developmental time given different numbers of age classes in a stage (Erlang parameter k) (see Fig. A1b).

Δx is the daily increment of physiological age computed using text equation 1, and

$\mu_i(t)$ is the proportional age-specific net-loss rate as modified by temperature, age, net immigration, and mortality due natural enemies (i.e., the biology outlined in the text).

All life stages of insect species n can be included in one dynamics model or each life stage may be modeled separately. Reproduction by the adult age classes entering the first age cohort of the egg stage $(N_{e,1}(t))$ as $x_{0,n}(t)$, with flows between stages $(y_{e,n}(t), y_{l,n}(t), y_{p,n}(t))$, and survivors exiting at maximum adult age as $y_n(t)$ (Fig. A1a). (By analogy,

births in plants would be the production of new plant or subunits.) Ignoring stage subscripts, the flow rate $(r_i(t))$ between age classes within a stage (Fig. A1b) depends on the number (mass) in the previous age class, k, stage Δ and Δx. The distribution of stage maturation times is determined by the number of age classes k and the variance of maturation times (var) (e.g., $k = \Delta^2/\text{var}$) (Fig. A1c). The larger the value of k, the narrower is the Erlang distribution of developmental times of cohort members. A value of $k = 25$ was selected that assumes an intermediate level of variability in developmental times for all species and sub-stages.